

# INSAR MONITORING OF THE LUSI MUD VOLCANO, EAST JAVA, FROM 2006 TO 2010

*Charlotte Gauchet, Emmanuel Christophe, Aik Song Chia, Tiangang Yin, Soo Chin Liew*

Centre for Remote Imaging, Sensing and Processing, National University of Singapore

## 1. INTRODUCTION

The Lusi mud volcano erupted on May 29<sup>th</sup>, 2006. A few months later, a gas pipeline exploded a few hundred metres to the North of the crater and killed 13 people. As the volcano is in the middle of a suburb of Sidoarjo, more than 30,000 people had to move elsewhere. The volcano is currently 20m deep with a surface area of about  $8km^2$ , despite the dykes built around it. The mud comes from a pocket of pressurized hot water about 2500 metres below the surface. When the water rises, it mixes with sediments to form the viscous mud. As the crater is close to important communication links and the Porong river, a trench has been dug to conduct the mud into the river. There are a lot of mud volcanoes in the world, some in East Java, but this is the first one whose birth has been seen and that has a very fast growth. Lusi could continue its mud eruption for years or even decades.

Synthetic-Aperture Radar (SAR) uses the motion of the antenna to get images with a very good spatial resolution. Microwave pulses are sent from a moving airplane or satellite to the ground and images are synthesized from the reflected signals. The images can be obtained regardless of the time and the weather. SAR interferometry (InSAR) uses the difference of phase between two complex-valued SAR images to provide the displacement of the ground, with a good accuracy. Interferometry processing is a topic well-explored [1] for more than a decade. To study Lusi, we used repeat-pass InSAR, with ALOS/PALSAR images.

The mission of the Japanese Advanced Land Observing Satellite (ALOS) is precise land coverage observation and disaster monitoring. Its third sensor is the Phased Array type L-band Synthetic Aperture Radar (PALSAR). The satellite has a repeat period of 46 days and an altitude of about  $700km$ . L-band corresponds to the most suitable wavelength currently available for tropical monitoring ( $\lambda = 23.6cm$ ).

## 2. PROCESS

ALOS has two interesting paths for Lusi monitoring: 430-7020 and 427-7030. InSAR studies on Lusi have already been done in 2006 and 2007[2], using the path 430-7020. This paper proposes to extend the study to the period 2006-2010. The process to study the volcano consists of several steps.

### SLC images

First of all, all information related to the ALOS images are obtained from the satellite website: path number, date, mode, direction of observation (ascending or descending), nadir angle (angle of observation) and latitudes and longitudes. The modes of interest to us are: Fine-Beam Single (FBS) for Single Polarisation and Fine-Beam Dual (FBD) for Dual Polarisation (HH+HV). It is very important to choose the same path, direction and nadir angle for all images because the first step, which is to gather the images, determines the accuracy. As images have both modes FBS and FBD, they need to be oversampled. And, as the satellite does not go exactly by the same path, it is also necessary to resample all images to the same frame. This frame corresponds to the global master image (called MASTER in this process).

The choice of MASTER is quite important as it defines both the frame for all future images and the baselines between this global master image and the other ones. To get a good accuracy it is necessary that no baseline is more than 15km. In the list of available images for the path 427, from 30 December 2006 to 25 August 2010, we chose 19 August 2008 as MASTER as it is near the mean date and the baselines with the other images were short.

The Digital Elevation Model (DEM) of MASTER will enable us to remove the elevation part from the phase to get only the displacement component (cf equation 1).

## Interferograms

Every interferogram is made from two images: one master (which does not correspond to MASTER) and one slave. The interferograms enable us to get the difference of phase between the two images and, at the end of the process, to get the displacement that occurred between the master and slave dates. Yet, as the phase contains several components, there are several steps to remove the unwanted components one by one.

$$\Phi = \Phi_{ele} + \Phi_{Ear} + \Phi_{atm} + \Phi_{bas} + \Phi_{dis} + \Phi_0 \quad (1)$$

$\Phi$  is the global phase image,  $\Phi_{ele}$  is the phase corresponding to the elevation,  $\Phi_{Ear}$  is the one corresponding to the Earth curvature,  $\Phi_{atm}$  to the atmosphere effects,  $\Phi_{bas}$  to the baseline effect,  $\Phi_{dis}$  is the phase corresponding to the displacement (the one we want), and  $\Phi_0$  is a constant (offset).

After having resampled all images on the MASTER frame, we can continue the process by creating interferograms from pairs of consecutive images: as we have 22 images for the path 427, it creates 21 interferograms. For that, we need to determine different kinds of offsets and calculate the baseline between the master and slave images. Once we have the first interferograms we have two choices: create the differential interferograms or only the flattening ones.

The flattening is very important because it deletes one of the unwanted components of the phase: the Earth phase contribution,  $\Phi_{Ear}$  in equation 1. It means that we take into account the Earth curvature at the study area and remove it.

The 2-pass method (with DEM) of processing differential interferometry uses the DEM as a reference to create an interferogram without elevation contribution. This interferogram has the same form as the first one but the elevation phase  $\Phi_{ele}$  and the Earth contribution (flattening)  $\Phi_{Ear}$  (cf equation 1) have been removed.

Until this step, all processes were at full resolution. To gain memory space and time, we divide (multi-looking) the size by 2 in range (image width) and by 5 in azimuth (image height). The proportions of the image looks better as the range and azimuth resolutions are now similar, but this oversampling reduces the quality of the images. Then, the filtering step is to reduce the noise in the image with an adaptive filtering based on the local fringe spectrum. Multi-looking and filtering are not compulsory but can help to make the final step easier.

Once all the other components have been removed, we get a wrapped phase: there are fringes on the image. Each cycle of fringes represents a period of  $2\pi$ . Thus the phase needs to be unwrapped to get values between  $-\infty$  and  $+\infty$  (cf fig 1).

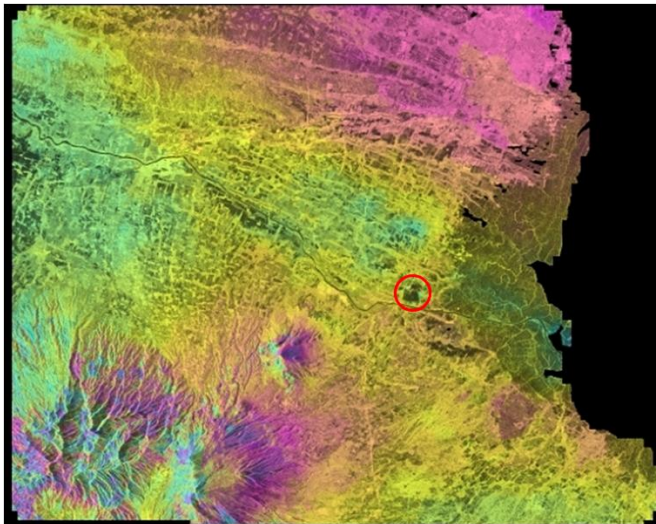


**Fig. 1.** The unwrapped interferogram 20061230-20070214 with path 427-7030. The volcano is located in the circled area.

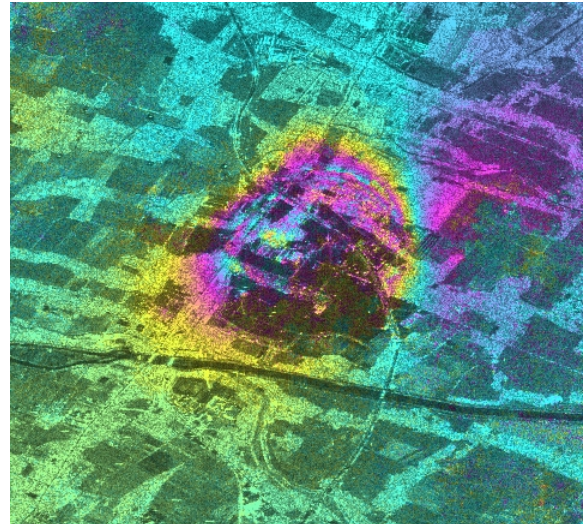


**Fig. 2.** Zoom on the volcano, interferogram 20061004-20060519 with path 430-7020.

### 3. OBTAINING THE MOTION

#### From unwrapped phase to motion

Unwrapping is the last step of the process which gives the displacement phase  $\Phi_{dis}$  (in equation 1). This phase, between  $-\infty$  and  $+\infty$ , is linked to the motion  $\Delta$  that occurred between the date of the master image and the slave image by the equation:

$$\Delta = \frac{\Phi_{dis} \times \lambda/2}{2\pi} \quad \text{with } \lambda = 23.6\text{cm} \quad (2)$$

Then, to get the motion on one point on the ground, we only need to know the phase of the corresponding pixel on the unwrapped interferogram image. As the phase is random for wet areas with L-band InSAR, points around the mud volcano were chosen to obtain graphs with their motion values over time. But sometimes values are too high or too low. That means that for these interferograms there are problems and the unwrapped phase does not correspond only to the displacement phase. This can be due to the atmospheric effects.

#### Atmospheric effects

To remove the atmospheric effects  $\Phi_{atm}$ , we can use stable points assuming that their phase is linear with the elevation. For that, a large list of resampled images is needed, because the more images are used, the more accurate the stable points are. This time, the pixel's amplitude is used instead of the phase. After assembling the set of amplitude files in a global image to get the amplitude mean  $m_{i,j}$  and variance  $\sigma_{i,j}$  for each pixel (cf equations 3 and 4), we can locate the stable points (cf fig 4) using the dispersion index  $D_{i,j}$ .

$$m_{i,j} = \frac{\sum_{i,j} A_{i,j}}{size} \quad (3)$$

$$\sigma_{i,j} = \frac{\sum_{i,j} A_{i,j}^2}{size^2} \quad (4)$$

$$D_{i,j} = \frac{\sigma_{i,j}}{m_{i,j}} \quad (5)$$

where *size* is the image size: line width  $\times$  column length.

The dispersion index  $D_{i,j}$  (cf equation 5) is a measure of the phase stability. As pixels with a high phase stability are needed to find the atmospheric effects,  $D_{i,j}$  has to be under a given threshold [3]. To not have too many points to generate, a threshold of 0.10 has been chosen.

Thus every pixel with a dispersion index under 0.15 is considered stable. Once all stable points are established, we draw them on the global image (cf fig 4). The colours indicate their density: red means that there are a lot of stable points gathered on the same area. They are often in the settled areas because the buildings are constant. This is confirmed in figure 4 where the stable points are located along the roads.

If the found points are very stable, it means that their displacement phases become negligible compared to  $\Phi_{dis}$  for the other points of the image, and hence the unwrapped phase associated with these points will be only effects. Thus, with these measured effects, and an equation over each image linking them together, they can be removed on the whole image to obtain the real displacements.

For each of the 21 interferograms, 3D graphs are drawn with the parameters: columns as X axis; lines as Y axis; unwrapped phase as Z axis. Finding the equation of the mean plane (cf equation 6) going through all the stable points will confirm if the atmospheric effects are proportional to the elevation or not.

$$Z = a \times X + b \times Y + c \quad (6)$$

After drawing both the stable points and the mean plane, the plane assumption revealed itself as not correct: many of the stable points are located far from the mean plane.

Doing this process for the whole list of interferograms shows that the atmosphere effects  $\Phi_{atm}$ , are not reduced to a linear relation with the elevation. Indeed, although SAR obtains images regardless of the time and the weather, clouds, smoke and other atmospheric events can delay the microwaves and distort the results.

### 4. RESULTS

Figure 2 is an example of the first qualitative results we got with the path 430-7020 [2]. This unwrapped interferogram shows that there is, at least between 19 May and 04 October 2006, an important displacement around the volcano. This is not surprising as the eruption occurred at the end of May 2006 and between the two dates, the mud covered several square kilometres.



**Fig. 3.** Lusi on September 26<sup>th</sup>, 2010.

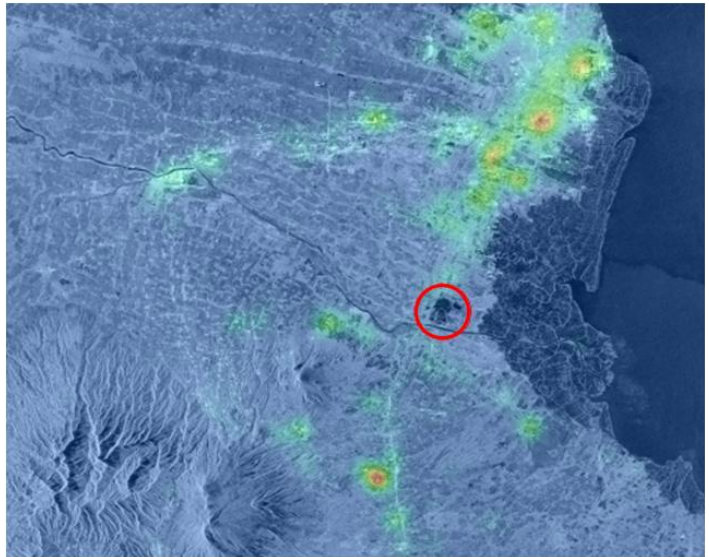


**Fig. 4.** Stable points density, threshold of 0.15.

Hence, with these convincing results, the process is continued to get the real values of the motion. For that, all the unwanted components of the phase (cf equation 1) are removed. Then stable points, not really close to the volcano, are chosen to obtain the displacements. They give the general evolution of the region, but in spite of very good dispersion indices, the motion on these points is not regular.

Finally, good results are found but for some dates there are baseline issues which give rise to wrong phase values and thus wrong displacements. Moreover, sometimes the displacement oscillates between positive and negative values for the same point over time, which is quite impossible: without a significant geological event, the ground does not move up and then down.

In conclusion, there is a general subsidence in this region [2], which must be due to the Lusi mud volcano: as the water from under the ground is released through the surface, the ground collapses on itself.

## 5. PERSPECTIVE

The process needs improvement to reduce the noise and effects still present in some unwrapped interferograms. The complete set of images from path 430 will be useful to compare the found displacements. By restricting the time span for the stability condition, points closer to the volcano could give useful results as they may be stable before being covered by mud.

The main problem of doing InSAR on Lusi is the kind of volcano we have to deal with: the mud on the volcano decreases the coherence and makes it impossible to get precise results on the volcano itself. The use of GPS data will enable an increase in the accuracy of the measurement and help to remove sources of noise [2].

## 6. REFERENCES

- [1] Richard Bamler and Philipp Hartl, "Synthetic aperture radar interferometry," *Inverse Problems*, vol. 14, 1998.
- [2] M.A. Kusuma H. Andreas T. Deguchi H.Z. Abidin, R.J. Davies, "Subsidence and uplift of Sidoarjo (East Java) due to the eruption of the Lusi mud volcano (2006-present)," *Environmental Geology*, , no. 57, pp. 833–844, 2009.
- [3] C. Prati A. Ferretti and F. Rocca, "Permanent Scatterers in SAR Interferometry," *IEEE Transactions on Geoscience and Remote Sensing*, vol. 39, no. 1, Jan 2001.